Assessment of the Methodology for Bounding Loran Temporal ASF for Aviation

Sherman C. Lo, *Stanford University*
Robert Wenzel, *Booz Allen Hamilton*
Greg Johnson, *Alion Science and Technology*
Per K. Enge, *Stanford University*

ABSTRACT

As we become increasingly dependent on GPS for many position, navigation, and time (PNT) applications, it becomes increasingly important that we have an alternate means of obtaining those capabilities. This is especially important in critical applications such as aviation. As part of the ongoing Federal Aviation Administration (FAA) Loran evaluation, the system is being assessed for its ability to provide stand alone navigation capability through all phases of flight. This will allow users to retain much of the functionality enjoyed when using GPS should the system become unavailable.

For Loran to be used for aviation navigation, it must meet strict integrity requirements. A key requisite for meeting integrity is the ability to bound position errors to a high degree of confidence. This, in turn, means bounding range domain errors and variations. One major source of variation is the temporal variation of propagation delay known as additional secondary factor or ASF. Models were developed to provide the bound on the ASF variations for the assessment of Loran aviation coverage. These bounds are designed to meet the integrity requirements on the error. Significant amounts of high quality Loran data from the U. S. Coast Guard (USCG) has been used to generate the model. This, however, left little data of adequate quality to perform the independent assessment of the models' performance. Hence, little or no independent validation of the efficacy of the bounds could be done until recently.

This paper presents an analysis of the models for bounding the temporal variation of ASF. It uses data collected in 2006 and 2007 from seasonal monitors installed by the FAA Loran evaluation team. It will examine both the performance of the bounds in the range and position domain. One major range domain bound issue examined is ensuring the ASF bound attributed to the uncorrelated component is adequate. This is important as the uncorrelated component is treated much more conservatively than the correlated component. Additionally, some sensitivity will be examined to test robustness of the model and implementation.

1.0 INTRODUCTION

Additional secondary factor (ASF) is the extra delay on the time of arrival (TOA) of the Loran signal due to propagation over a nonhomogenous land path vice an all seawater path. This delay can be significant and will result in position errors of hundreds of meters or more should it not be accounted for. As such, reasonable estimates of ASF are necessary for accurate positioning using Loran. The upshot is that most modern receivers utilize a static estimate of ASF. However, even with good ASF estimates, significant position errors may result as the ASF varies temporally. The temporal variation of ASF can be on the order of half a kilometer over the course of a year. This represents the largest source of error on Loran.

Properly accounting for the effects of ASF is necessary for supporting the use of Loran for aircraft navigation and landing. This application is a primary goal of enhanced Loran (*eLoran*), the next generation of Loran. To support aircraft landing, *eLoran* will have to meet the requirements of non-precision approach (NPA) operations such as LNAV, which permits a 350 ft decision height [1][2][3]. Meeting the integrity requirements means that the position errors are bounded to a high confidence level. This requires that each error source is adequately bounded. As the temporal variation of ASF is the largest such error source, it is critical to overbound this error. However, the bound cannot be too excessive as it would make the system unavailable for the desired operation.

As such, the Federal Aviation Administration (FAA) Loran Technical Evaluation team has developed models for bounding the temporal variation of ASF. This paper details the analysis of data supporting the validation of these models. The first section of the paper will discuss background on the temporal ASF variation bound

methodology and models. The next section will describe the source and collection of the data used for the assessment. The body of the paper will compare the collected ASF and its resultant model bound. It will examine this in the range domain and project that comparison to the position domain. The paper will also assess the sensitivity of the model to specific errors and variations to ensure robust performance.

2.0 BACKGROUND

The section describes the methodology used to bound the temporal ASF variations. The methodology requires two components – an estimate of the seasonal midpoint value of ASF and a model that bounds the peak to peak temporal ASF variation. The seasonal midpoint represents the nominal ASF that the user receiver applies. It is about this nominal value that the bound is applicable. These two parts are illustrated in Figure 1. The Loran evaluation team is still working on its preferred methodology for determining the seasonal midpoint and this portion will not be discussed. The models developed to bound the peak to peak temporal ASF variation will be described later in this section. The description and analysis of the performance the models is the focus of the paper.

2.1 BOUNDING TEMPORAL ASF VARIATION

A methodology for bounding the temporal variation of ASF was developed to support the use of Loran for NPA. The assumption is that the receiver would store and apply some nominal value (or values) of ASF as well as the associated temporal ASF bound or bounds. Application of this nominal value results in a residual or corrected ASF (*ASFc*). The temporal ASF bound ($ASFbound_{temp}$) would bound the maximum excursion from this value. This is just the maximum absolute value of *ASFc*. Using the seasonal midpoint ASF ($ASF_{temp,midpt}$), as defined by Equation 1, results in the smallest possible temporal ASF bound. The basic premise is seen Figure 1. A nominal value of ASF and the associated bound(s) that is applicable for the entire year is assumed to be used. This is because analysis suggests when we have to protect the integrity of the worst case, there is little advantage in using different nominal values during the year [4]. The reason for this is that winter variations can span much of the entire range. So bounding the winter essentially requires bounding the entire yearly range.

Define:

$$ASF(t) = ASFc(t) + ASF_{temp,midpt} \quad \text{and}$$

$$ASF_{temp}^{peak-peak} = \max\left(ASF(t)\right) - \min\left(ASF(t)\right)$$

$$ASF_{temp,midpt} = \frac{1}{2}\left(\max\left(ASF(t)\right) + \min\left(ASF(t)\right)\right) \quad (1)$$

Equation 2 expresses the requirement for a simple, one term temporal ASF bound. If we wish to ensure an adequate position domain bound, we need to make sure that the temporal ASF bounds for the signals used are combined in a conservative manner. Since only one term per signal is used to bound, we have to assume the worst case relationship between the bound of each signal. The conservatism results in a very conservative horizontal protection level (HPL) which is the bound on horizontal position error (HPE).

$$\begin{aligned} &\tfrac{1}{2}\left(\max\left(ASF(t)\right) - \min\left(ASF(t)\right)\right) \\ &= \tfrac{1}{2}\, ASF_{temp}^{peak-peak} \le ASFbound_{temp} \end{aligned} \quad (2)$$

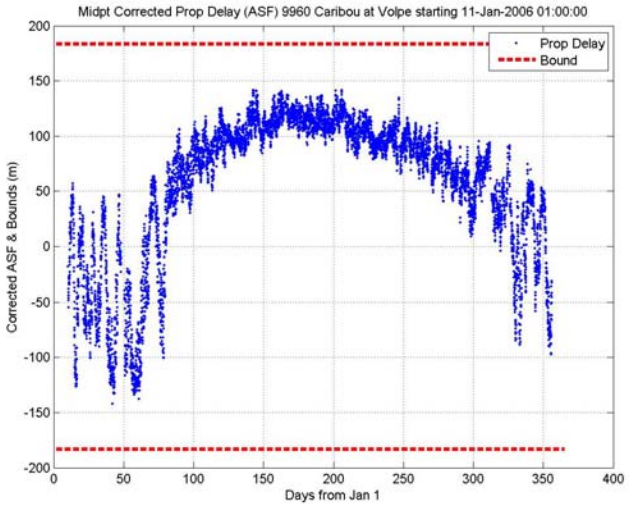

Figure 1. Example showing total bound on temporal ASF variation and estimated Midpoint ASF

2.2 COMPONENTS OF TEMPORAL ASF VARIATION

Dividing the bound into different components can reduce conservatism. Different forms of error are affected differently by the position solution. For example, error or variations common to all measurements essentially do not affect the position solution. The cumulative effect of common mode errors, meaning errors that are the same on all signals, is calculated by the traditional navigation least squared solution used by Loran and GNSS along with the position. It is only the residual variations after removing the common terms that affect the position solution. In addition to common error, the variation can be further divided into different categories. We can create bounds for each category so that the overall combination will bound in the position domain. In our model, the bound

variation is separated into two components: correlated and uncorrelated.

The correlated ASF is the portion of the temporal ASF seasonal variation that is related to path length. As such, it can be considered to move in a similar direction for all received signals. In calculating the HPL, the correlated ASF bound can be combined using the known correlation. The uncorrelated temporal ASF is the residual error. It is the portion of the temporal ASF that cannot be considered to move in a similar direction as all other signals. Only this portion must be treated in the worst case combination. The division allows for some of the ASF bound variation to be treated in a related manner rather than in the worst case combination. Physics suggest that the division is realistic as some of the ASF variation between different signals is correlated as they share some common weather and land regions. The properties of the propagation region determine the ASF. This separation into these two components also has historical precedent dating to work by Johler and Doherty [5][6]. Two basic models were developed and their development is described in [4]. This is discussed in the next session.

Given the division, how do we ensure that the bound results in a sufficient HPL? If the true correlated ($ASFc_{corr}$), uncorrelated ($ASFc_{uncorr}$) and common components of ASF are known, a sufficiency condition can be derived. First, we should have the uncorrelated portion of ASF completely bounded by the uncorrelated bound. Second, we need the correlated portion of ASF bounded. This is done by the combination of the correlated bound and the portion of the uncorrelated bound not used to meet the previous requirement. These conditions are expressed in Equations 3 and 4 which state: 1) the uncorrelated bound should overbound the maximum uncorrelated ASF and 2) the total bound should bound the total of the correlated and uncorrelated component, respectively.

$$\max\left(\left|ASFc_{uncorr}(t)\right|\right) \le ASFbound_{temp,uncorr} \tag{3}$$

$$\max\left(\left|ASFc_{uncorr}(t) + ASFc_{corr}(t)\right|\right) \le \left(ASFbound_{temp,corr} + ASFbound_{temp,uncorr}\right) \tag{4}$$

However, if the components of ASF are not known, a condition such as given in Equation 5 can only provide confidence but not assurance that the position domain is protected.

$$\left|ASF_{temp}(t) - ASF_{temp,midpt}\right| = \tfrac{1}{2} ASF_{temp}^{peak-peak} \le \left(ASFbound_{temp,corr} + ASFbound_{temp,uncorr} + common\right) \tag{5}$$

2.3 TEMPORAL ASF VARIATION BOUND MODELS

This section describes the models developed and used by the Loran evaluation team. Two basic models are described: the model used for the 2004 evaluation report and the improved model based on weather data.

2.3.1 MODELS FOR 2004 REPORT

For the 2004 FAA technical evaluation [1], a bound model was developed to determine Loran NPA LNAV coverage. Past Loran data and studies were used as the basis of this model. Specifically, the NEUS/SEUS (1983) and West Coast (1986) signal stability reports were used [7][8]. As there was no mid-continent data in the 1980s (and hence it was not studied), 2002-2003 Loran Operations Information System (LOIS) data was analyzed to provide values for the mid-continent. The goal of these historical (1980s) studies was not to determine a bound but rather to determine the best ASF to use and statistics on the variation of ASF. Accordingly, some analysis and reinterpretations of those results were necessary. This model is termed the 2004 intended model. In the process of incorporating the model into the Loran aviation coverage tool [2], the calculation of the uncorrelated term changed, resulting in a slightly less conservative bound. This altered model was used in the 2004 report and will be termed the 2004 report model or Model 1 for the purpose of discussion. Model 1 will be examined in this paper as it was used to initially determine *eLoran* NPA coverage.

2.3.2 WEATHER REGRESSION MODEL

After the 2004 report, it was felt that the 2004 model lacked the desired resolution and preciseness. Additionally, it was hoped that some of the conservatism of the model could be reduced. And so, a model based on high density weather data was developed. The model is based on the dry component of index of refraction (N_{dry}), a term that is known to be correlated with changes in Loran propagation speed [9]. A map for generating the temporal ASF bound was developed based on weather measurements from over 1400 National Oceanic Atmospheric Administration (NOAA) sites. For this paper, we term this model the weather regression model or Model 3. While Models 1 and 3 are examined in this paper, the focus will be on Model 3 since it will likely be the model used operationally due to its better resolution.

2.4 CALCULATING MODEL BOUNDS FROM MAP

Both models output the correlated and uncorrelated bounds for the temporal ASF variation. The models are essentially used in a similar manner to generate the bounds; however, the underlying maps for weighting the

effect of propagation path are different between baseline models. The calculation starts by taking an integral over the path between the user and the transmitter used. This integral is weighted by the underlying map values. Denote the value of the integral as *d*. This value is then used to derive the correlated and uncorrelated bound. Since the underlying maps for the 2004 model and the weather regression model are different, the integral will result in different values.

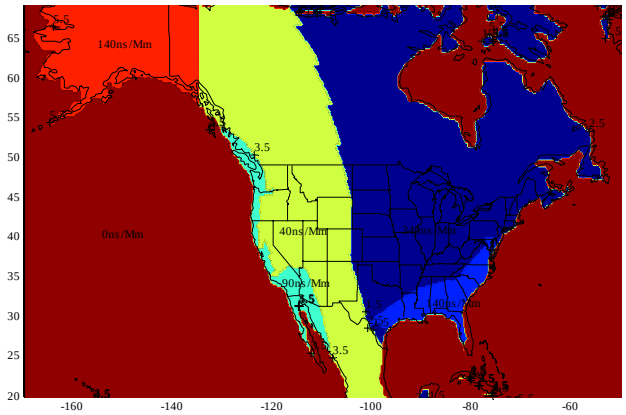

Figure 2. Map of Different Regions Affecting Temporal ASF Variations for 2004 Models

Region	Corr (σ_{dTD}) (ns/Mm)	Uncorr (report) (ns/Mm)	Uncorr (revised) (ns)
1	0	0	0
2	40	200	200
3	90	100	100
4	140	150	150
5	340	250	250

Table 1. Regional Weights for Correlated and Uncorrelated Temporal ASF for 2004 Models

The map for the 2004 models relating the relative propagation path effects on temporal ASF variation is seen in Figure 2. The values shown on the map are related to the correlated component. While the values may be different, the correlated and uncorrelated models utilize the same regional divisions. Determination of the correlated portion is calculated by taking the path integral over the map using the values in each region. The result is a root mean squared (rms) value of the temporal variation/deviation. We multiplied by a factor of 2.95 to transform the rms value to an absolute bound, where the factor of 2.95 was derived empirically. Determination of the uncorrelated component uses the same map though the values for the regions are different. This is seen in Table 1. As mentioned, the 2004 intended model was altered when implemented in the coverage tool. The only difference between the report and intended model is with the calculation of the uncorrelated component. The uncorrelated component was meant to be fixed term regardless of path length. If the path traverses several regions, the uncorrelated component is the fixed component of the regions weighted by the percentage of path in those regions. Mathematically, it is calculated as the sum of the fixed value for those regions multiplied by the percentage of the path in those regions.

The calculation of the correlated and uncorrelated components of ASF variation using the weather regression model is reasonably straight forward. Using the map seen in Figure 3, the correlated and uncorrelated components are calculated using Equations 6 and 7, respectively.

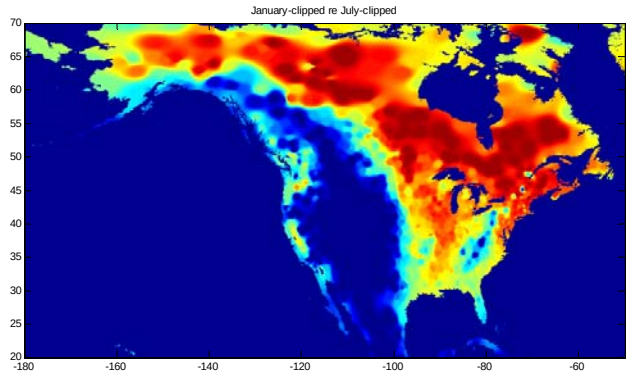

Figure 3. Map of Different Regions Affecting Temporal ASF Variations for Weather Model

Correlated ASF bound=3.0636*d μsec=0.9184*d m (6)

$$ASF_{uncorr,\max} = 1.32\sqrt{\frac{d+16.36}{1636.905}}\mu\sec \quad (7)$$

	Report 2004 (Model 1)	Intended 2004 (Model 2)	Weather Regression (Model 3)
Correlated Bound (μsec)	2.95*d/1000 μsec	2.95*d/1000 μsec	3.0636*d μsec
	0.8824*d m	0.8824*d m	918.4*d m
Uncorrelated Bound (μsec)	d*/1000 μsec where d* is path integral using uncorrelated weights	d'/1000 μsec where d' is path percentage weighted value of uncorrelated bias	$1.32\sqrt{\frac{d+16.36}{1636.905}}$ μsec
	0.29979*d*	0.29979*d'	$395.7\sqrt{\frac{d+16.36}{1636.905}}$ m

Table 2. Calculation of Correlated & Uncorrelated Temporal ASF Variation (3 Models)

2.5 DATA FOR ASSESSMENT

While the US Coast Guard (USCG) has gathered significant data on Loran over the past years, there is a need for additional data for validation. Part of the reason

is due to the fact that the USCG data was used to develop the models. For example, data from USCG LRS IIID Loran receivers taken between May 2003 and September 2004 was used to develop the relationship between N_{dry} and ASF (Time Interval Number (TINO) data taken from Remote Automated Integrated Loran (RAIL)). Additionally, there is a need for a data source from which we can directly measure ASF with minimal contamination from other sources of TOA variations.

As part of the FAA evaluation, seasonal Loran monitors were set up throughout the Northeast United States. The monitors located in Boston (Volpe National Transportation Center), MA, University of Rhode Island (URI), RI, US Coast Guard Academy (USCGA), New London, CT, Ohio University, Athens, OH, and Atlantic City, NJ. Additional monitors were installed in the Northeast in 2007. These seasonal monitors provide data to support the evaluation including differential Loran and the ASF evaluation. In this paper, we will focus mostly on data from 2006. A few results from 2007 will be included. However, we are still processing the data and examining outliers.

The raw data has outliers and other discontinuities and variations not related to ASF due to installation, processing or other factors. The data was processed to remove obvious outliers using some automatic filter rules. However some outliers remain as we want to retain as much of the true ASF variation as possible. Additionally, there is noise in the measurements. For example, the 2006 USCGA data had significant noise due to a local noise source. The monitor has now been moved. While the data is averaged to reduce noise, it is not eliminated and represents an additional error. Details on the monitors and data processing are given in [10][11].

2.6 CALCULATING HPL BOUNDS

The Loran integrity or HPL equation is given in Equation 8. This equation governs the bounding of the horizontal position error of which the contribution of the temporal variation of ASF is only a component. Of interest to the bounding of the temporal variation are the second and third terms of the equation which deal with how to add correlated and uncorrelated biases.

$$HPL = \kappa \sqrt{\sum_i K_i \alpha_i^2} + \left| \sum_i K_i \beta_i \right| + \sum_i \left| K_i \gamma_i \right| + PB \qquad (8)$$

The second term of the equation relates to completely correlated biases. This is used to bound the temporal variation in ASF that is correlated with our weighted land path integral discussed in Section 2.2. Since these errors are correlated, the confidence bounds for these errors can be added together before taking the absolute maximum. In other words, because of the correlation, we do not have to take the worst-case combination. When examining the temporal variations, β represents the absolute bound on the correlated component.

The third term accounts for bias errors that are uncorrelated. The confidence bounds, γ, for these errors must be added together in the worst-case combination. For the temporal variations, γ represents the absolute bound on the correlated component.

The matrix K comes from the weighted least-squares pseudoinverse matrix that determines the position solution. It is derived from the geometry matrix G which relates pseudorange measurements (y) to the position solution (x) and the weighting matrix, W, used to weigh the relative confidence of each pseudorange measurement. This seen in Equations 9 and 10.

$$\hat{x} = (G^T W G)^{-1} G^T W y \equiv K y \qquad (9)$$

$$y = Gx + \varepsilon \qquad (10)$$

Hence the contribution of the temporal variation of ASF to the HPL is given by Equation 11. In Equation 11, β_i and γ_i represent the absolute bound on the correlated and uncorrelated component of the temporal variation of ASF for station i.

$$HPL_{tempASF} = \left| \sum_i K_i \beta_i \right| + \sum_i \left| K_i \gamma_i \right| \qquad (11)$$

3.0 ASSESSING THE MODEL BOUND: RANGE DOMAIN

For the analysis of the model bound performance in the range domain, we conducted two studies:

1) Comparison of the calculated corrected ASF with the correlated and uncorrelated ASF bound (Section 3.1)

2) Comparison of the maximum estimated correlated and uncorrelated components the temporal variation in ASF to their corresponding bounds (Section 3.2-3.3)

3.1 ASF VARIATION VS MODEL BOUND: OVERALL TOTAL

After filtering the data, we can compare the ASF variation to the bounds derived by the models. First, we begin be calculating the midpoint ASF value for each station used.

That point is set to be our nominal zero ASF error value. Centering the data, we can compare the result to the correlated, uncorrelated and total temporal ASF bound. An example of this for the Seneca signal as seen at Volpe using the Weather Regression Model is seen in Figure 4. As seen in the figure, some outliers remain (e.g. circa day 270). This is because the goal of the filtering is to remove obvious outliers while retaining the maximum true variation. If the filtering is too aggressive, some of the true variation may be lost.

The comparison is only a basic examination of the bound. It is straightforward and does not require estimates whose values may be dependent on the station set used for the estimation. It tests Equation 5 from Section 2.2. However, as discussed in that section, the analysis cannot guarantee that the bounds are adequate.

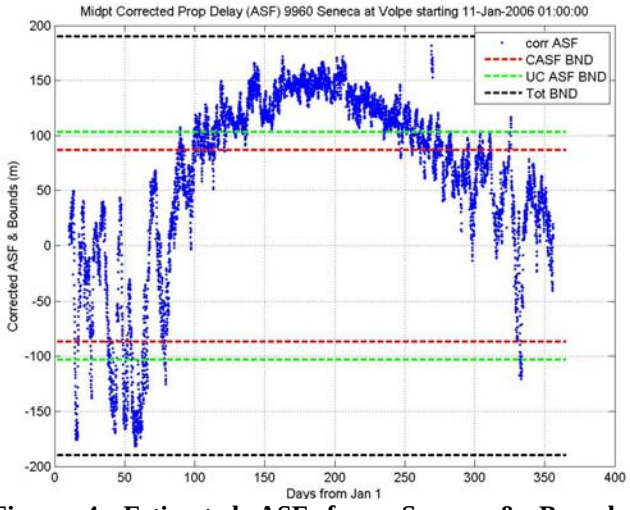

Figure 4. Estimated ASF from Seneca & Bound (Weather Model) as measured at Volpe, MA (2006)

In most cases examined, the total bound is larger than the maximum variations. Figure 5 shows the results for the Seneca, NY signals as measured by four seasonal monitor stations. The charts compare the bounds for correlated and uncorrelated ASF to the maximum error (deviation from the midpoint) over the course of 2006.

There are some cases in which the bounds are not larger than the maximum error. Usually, this occurs for nearby transmitters. Measurement noise and map coarseness are two likely causes of the results. Measurement noise can cause the maximum error to exceed the maximum ASF variation. Map coarseness can result in an inaccurate bound calculation. This may result in a smaller bound than expected. These two effects can be particularly significant when the location is near the transmitter.
When close to the transmitter, measurement noise generally contributes a greater fraction of the total measurement error than when further away. The dominant measurement noise when near the transmitter is due to transmitter jitter which is not path dependent. Hence, the ASF variation is less visible when near the transmitter.

The map coarseness can cause the bound to be different than what would be calculated using a more precise map. Additionally, transmitter and monitor locations are rounded to the nearest quarter degree. These two resolution related factors can result in a lower bound by treating a path as seawater when it is actually land. The effect is more pronounced at short distances. Nantucket, which is close to three of the monitor sites, illustrates this point. The results from Figure 7 show that both models produce total bounds that are less than the maximum variations. The 2004 report model treats the Nantucket signal at Volpe as having an all seawater path when this is not the case (as seen in Figure 6). Another indirect confirmation of the effect of map coarseness is provided by examining the results of the weather regression model. This model map is less coarse. This may explain why the bounds for the weather regression model are far larger than and much closer to the maximum error when compared to the 2004 model for Nantucket. As discussed next, the total bounds from the 2004 model are generally larger than the total bounds from the weather model.

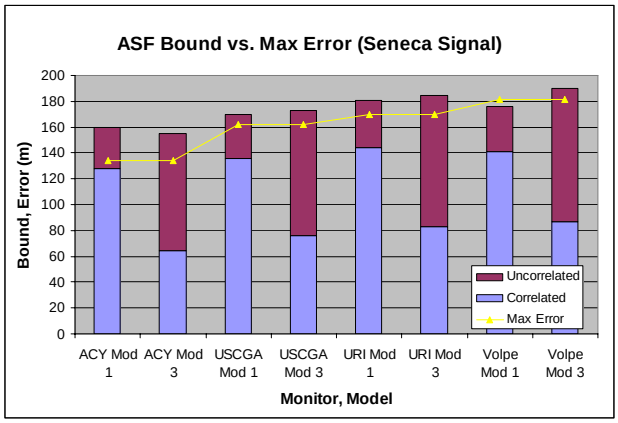

Figure 5. Temporal ASF Bound vs. Max Error: Seneca, NY Signal at 4 Monitor Sites (2006)

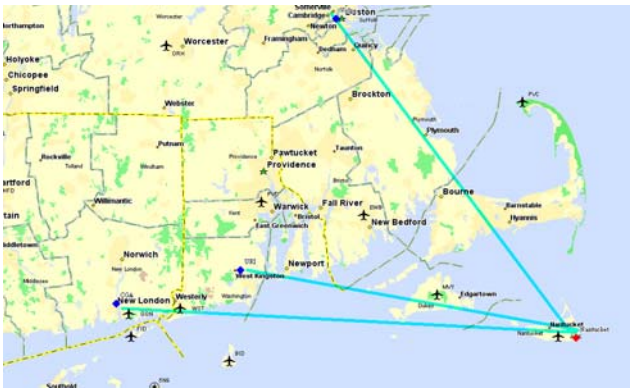

Figure 6. Propagation paths for the Nantucket Signal to USCGA, URI, and Volpe (West to East)

In comparing the two models, it is clear that the Model 1 generally has a higher total bound but a smaller uncorrelated component bound. This is again seen in Figure 8 which presents the bounds and the corresponding maximum ASF error at Ohio University in 2006. As will be seen later, the uncorrelated bound has a much greater effect on HPL and Model 3 invariably has a larger HPL even though its total bound is smaller.

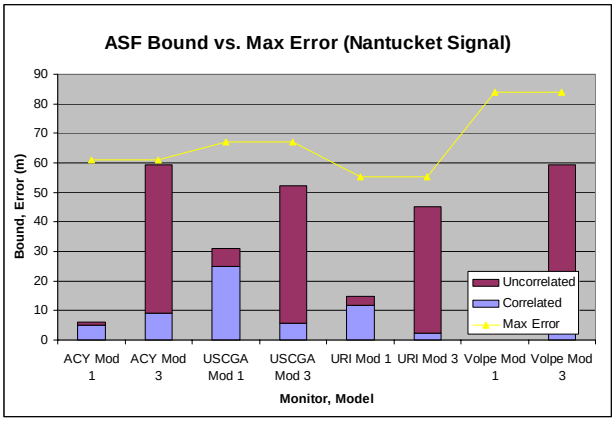

Figure 7. Temporal ASF Bound vs. Max Error: Nantucket, ME Signal at 4 Monitor Sites (2006)

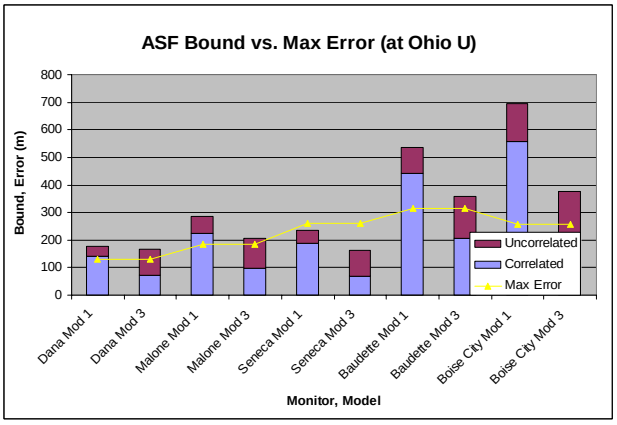

Figure 8. Comparison of Max. Error, 2004 Report & Weather Regression Model Bounds at OU (2006)

3.2 BOUND VS ACTUAL ASF COMPONENTS

A better sense of the sufficiency of bounds is gained by examining the distribution of the correlated and uncorrelated components of the ASF variation relative to their respective bounds. However, we cannot get these components directly as they arise from a mathematical simplification of the physical phenomenon. So, we estimate them from the ASF measurements. Using the corrected ASF (ASFc), we can estimate the common, correlated and uncorrelated components using least squares. The correlated term is related to the weighted land path *d* (using the map).

$$ASFc = y = ASF_{common} + ASF_{corr} + ASF_{uncorr}$$

$$ASF_{corr} = k_{corr,est} * d$$

$$\hat{x} = \begin{bmatrix} k_{corr,est} \\ ASF_{common} \end{bmatrix} \qquad H = \begin{bmatrix} d_1 & 1 \\ \vdots & \vdots \\ d_N & 1 \end{bmatrix}$$

$$y = Hx$$

$$\hat{x} = (H^T H)^{-1} H^T y \equiv Ky$$

$$ASF_{corr,normalized} = \frac{k_{corr,est} * d}{k_{\text{model}} * d} = \frac{k_{corr,est}}{k_{\text{model}}} \quad \textbf{(12)}$$

Now that the components have been estimated from measurements, we can compare them with their respective component bounds. We can examine the common and correlated term for all stations. The correlated component is related to each measurement by the corresponding weighted land path, *d*, multiplied by a common (to all measurements) factor, k_{corr}. Likewise the bound is related to *d* by a factor, k_{model}. Hence we compare the correlated term by just comparing the ratio of the k_{corr} factor determined from the data and the factor from the model. We term this ratio the normalized correlation factor. It is given in Equation 12. Figure 9 presents the normalized correlation factor along with the common term.

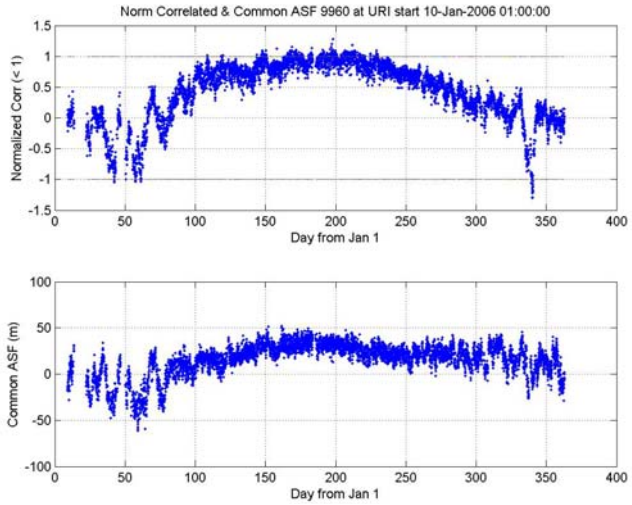

Figure 9. Estimated correlated component normalized by correlated bound (top) and common ASF (bottom) for 9960 signals at URI (2006)

The estimated uncorrelated component of ASF is compared to its respective bounds for each station used. This is seen in Figure 10.

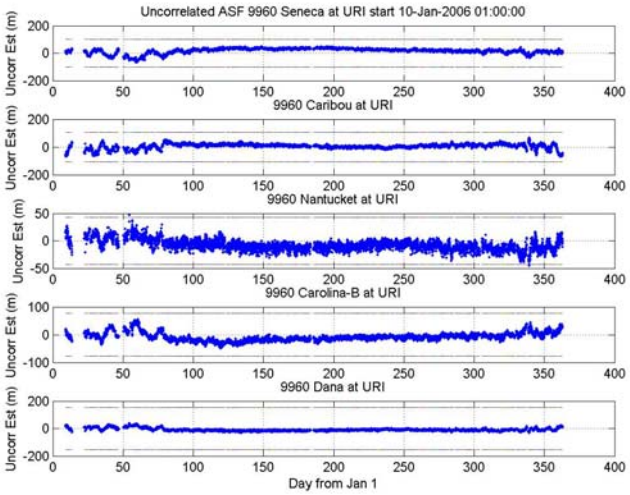

Figure 10. Estimated uncorrelated ASF component for 9960 signals at URI (2006)

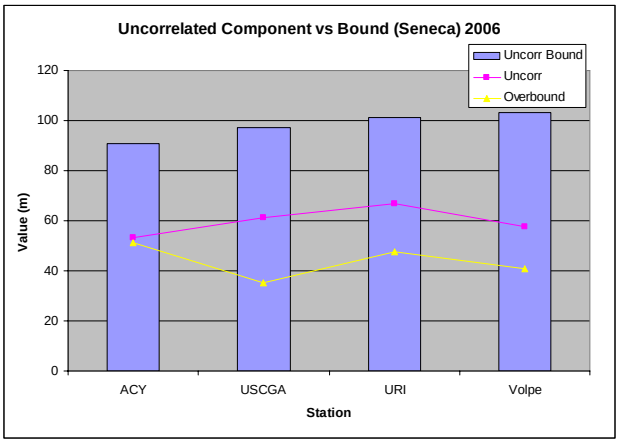

Figure 11. Comparison of Uncorrelated Bound to Estimated Uncorrelated Error and Difference between total bound and total error (2006)

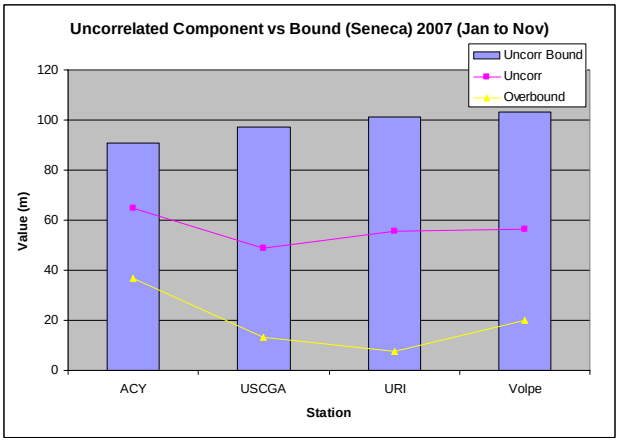

Figure 12. Comparison of Uncorrelated Bound to Estimated Uncorrelated Error and Difference between total bound and total error (2007)

The result can be more readily seen in Figure 11 and Figure 12. It helps show whether our two conditions for having an adequate bound are met. These conditions, as expressed in Equations 3 and 4, are that the uncorrelated bound should overbound the maximum uncorrelated ASF and that the total bound should bound the total of the correlated and uncorrelated component of ASF. The first condition is met if the uncorrelated bound is greater than maximum estimated uncorrelated component. The second condition is met if the overbound, which is the difference between the total bound and the maximum sum of the estimated correlated and uncorrelated components, is positive. The conditions are generally met however, there are some exceptions. For the 2006 data, exceptions are the same as noted previous, i.e. Nantucket signal when close to monitor site and noisy USCGA data. The overall results for all monitor sites in 2006 presented in Table 3. It presents the outcomes of the test of whether condition 1 and 2 are met. The results are given in meters and a positive value indicates the condition has been met. The only cases where the conditions are not met occur due to issues not attributable to ASF. For 2007, a few more cases exist where the conditions are not met. The result is likely due to the fact that we have not removed some of the non-ASF related outliers from the 2007 data.

Monitor	Cond.	Seneca	Caribou	Nantucket	Carolina	Dana
Atlantic City	1	37.52	66.27	13.82	46.74	61.49
	2	51.30	134.78	27.44	84.98	112.92
URI	1	34.23	39.05	-4.33	22.18	114.35
	2	47.70	80.18	-2.57	75.38	79.81
USCGA	1	36.20	14.32	-9.44	-6.55	77.92
	2	35.18	49.82	-2.44	29.94	52.87
Volpe	1	45.40	26.35	7.83	40.74	128.09
	2	40.70	78.94	6.84	73.47	50.54

Table 3. Test of Conditions 1: Uncorrelated Bound – Max Uncorrelated Component (m) & Condition 2: Total Bound – Max Correlated + Uncorrelated Components (m) using 2006 Data

3.3 SENSITIVITY

The estimated values of common, correlated, and uncorrelated components are sensitive to the stations used in the calculation. Ideally, there would be no dependency on the stations used. A dependency does exist because the model is not a perfect representation of the physics and there is noise in the measurement. As such, the estimates depend on the stations used in the calculation. If a different set of stations are used, different values will result. Regardless of what station set is used, the bounds still need to be adequate. To test that, we look at station subsets for each site and examine whether the bound indeed does still hold. In the previous analysis, the components are estimated using the five stations of the

primary chain at each location. In the first cut sensitivity analysis, we look at all combinations of four stations. Figure 13 shows an example of the results where we compare the estimate of the uncorrelated component of each station for each of the five combinations and the base (all five stations) case. The figure also includes the uncorrelated bound to see if the first condition of bounding the uncorrelated component is met.

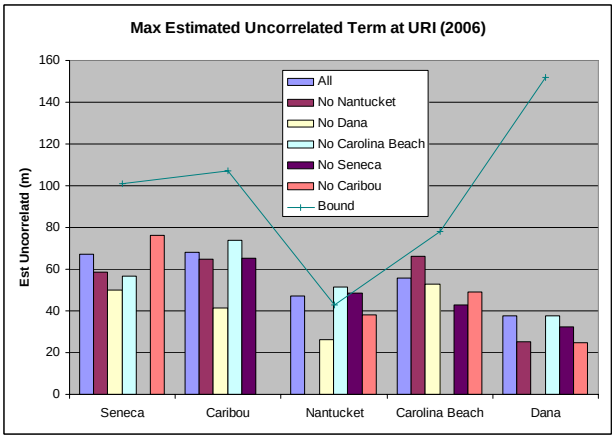

Figure 13. Estimated uncorrelated ASF component for each signal at URI for all 4 station subsets.

The results show that the maximum of estimated components are reasonably similar for the different sets examined and the bounds generally hold. The bound does not hold in a few cases. Equation 1 is met with the exception of the measurements Nantucket signal at URI or USCGA and Carolina Beach signal at USCGA. Variations not attributable to ASF are known to have a more significant affect on these cases. This is likely the cause for the slight underbound. Condition 2 is also usually met. When it is not met, the sum of the component error is only underbounded by less than 10 meters.

4.0 ASSESSING THE MODEL BOUND: POSITION DOMAIN

The most important demonstration is to show that position error due to temporal ASF can be bounded by its associated HPL. The HPE due to ASF is calculated using Equation 13 where ε is the deviation of ASF from the midpoint value for all stations. One implicit assumption from this step is that the midpoint ASF values used for each station measurement represents the zero position error value. This assumption may in fact be incorrect. The sensitivity of our result will be examined in the next section. The result of the calculation using Equation 13 is the position domain error vector, E. The vector E gives our errors in the horizontal plane as well as the clock error. Figure 15 shows the result of the calculation over the course of 2006 for Volpe using the 2004 Report Model. The HPL is calculated using Equation (11) applied to the ASF bound components. Both these results are sensitive to the weighting matrix, W, used. Two weightings were discussed in [12]. The analysis uses the preferred weighting in that paper. This weighting is based solely on the random component of error. The other possible weighting uses the random term plus the bias.

$$E = K\varepsilon \qquad (13)$$

We had previously engaged in this process for assessing the 2004 report model. We utilized USCG TINO data from May 2003 to September 2004 taken from Loran monitor receivers (Locus LRS IIID). This data is independent from source for validating the 2004 model. These cases are discussed in [4]. This data was later used to derive the weather regression model.

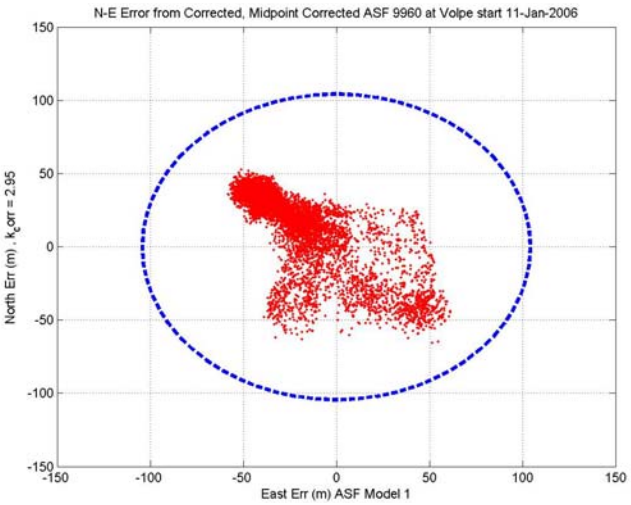

Figure 14. Scatter Plot of Position Errors and HPL in 2006 from Temporal ASF at Volpe, MA using 2004 Report Model

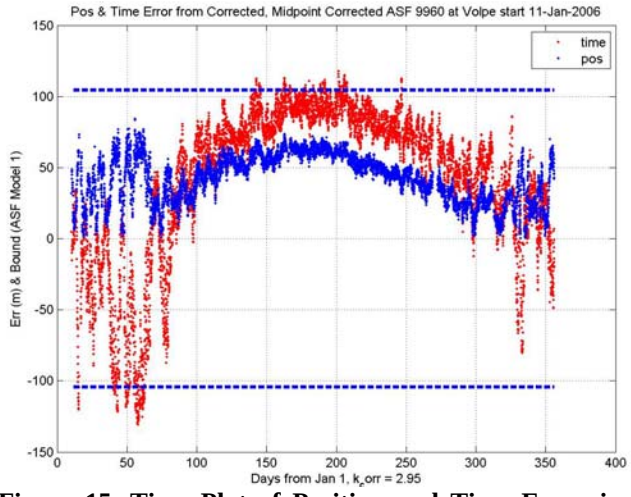

Figure 15. Time Plot of Position and Time Error in 2006 along with HPL Bound from Temporal ASF at Volpe, MA using 2004 Report Model

4.1 SUMMARY AND OBSERVATIONS

Table 4 shows a summary of the position bound generated for each model at each seasonal monitor site. Compared to those bounds is the maximum nominal (no error in midpoint estimation) error. As seen, the model bounds easily bound the maximum error with the weather regression model being more conservative in all cases. This is despite the fact that with the exception of close stations like Nantucket or measurements affected by map coarseness, the 2004 Report model bounds are generally larger than those of weather regression model. This can be seen in Figure 8 which compares the bounds at Ohio. For all total bounds, the 2004 report model is larger than the weather regression model. As seen in the table, the position domain bound from the weather model is nearly 45% larger than the 2004 model. The difference is due to the fact that the weather model has larger uncorrelated bias bounds. This emphasizes the importance of the uncorrelated bound as dominating the bound in the position domain.

Location	Volpe	URI	USCGA	Atlantic City	Ohio U
Model 1 (HPL)	104.1747	151.7882	180.0869	122.5328	132.3718
Model 3 (HPL)	148.4193	195.0466	222.1352	156.4173	191.4638
Max Err (Nom)	84.4826	100.9524	141.9671	82.6268	100.2864
Max Err (10%)	100.007	118.9679	166.195	97.6874	129.7506

Table 4. Summary of HPL from Temporal ASF Models, Maximum Error, & Max Error with Worst 10% Midpoint ASF Estimation Error at Monitor Sites (2006)

4.2 SENSITIVITY TO ERRORS IN ESTIMATING MIDPOINT

The model bounds assumed that the seasonal midpoint values of ASF are known and accurate. However, it is likely that our determination of the seasonal midpoint will have some errors. We can use the seasonal monitor data to get a first cut at how large the uncertainty can be while still bounding the position domain error. Error in the seasonal midpoint estimate was introduced to see its effects. The error in the estimate was taken as a percentage of the overall peak to peak value. Additionally, the worst combination of the error was selected. This means that relative sign on the error for each station was chosen so that the overall combination would result in the largest possible position error. Our analysis showed that a 10% error was acceptable for all of the monitor sites examined. Figure 16 shows an example result for Volpe using the weather model with a 10% error on each midpoint estimate chosen to add in the worst case manner. Table 4 shows the comparison of the bound to the maximum error for the nominal case and the case with 10% error in the midpoint estimate.

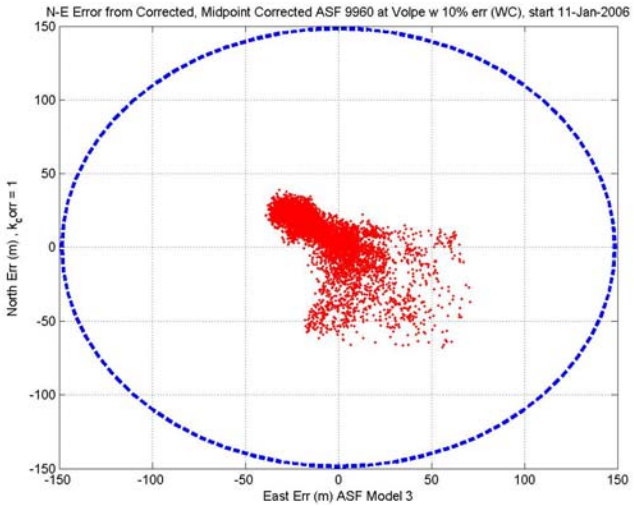

Figure 16. Position Domain Error for Volpe in 2006 using the Weather Model with 10% error in midpoint ASF estimate chosen to add in the worst manner

4.3 SENSITIVITY TO STATION SET AND OTHER FACTORS

We also want to make sure that the HPL bound is valid regardless of the station set used. To test the effect of station set used, we examined the HPL generated using the Model 3 bounds for every four-station subset combinations. In all cases, the HPL greatly overbounded the HPE. In approximately half of the cases, maximum HPE was less than 50% of the HPL. In the worst case, the maximum HPE was approximately 75% of HPL. The results generally indicate that the HPL is effective for all sets that a receiver is likely to use.

Preliminary analysis on the effects of using the other weight discussed in [12] shows that different HPL and maximum HPE result. However, the HPL was found to bound the HPE in all cases examined. In some cases, the HPL and maximum HPE were larger while in others they were smaller. If the previously discussed conditions 1 and 2 are met, the HPL should bound the HPE due to ASF regardless of weighting selected.

5.0 CONCLUSIONS

The goal of the Loran integrity performance panel (LORIPP), the multi-organizational team charged with assessing Loran for aviation, is to provide the necessary models and proofs to support aviation certification. Bounding the ASF variation is of great importance as it is one of the largest sources of measurement variation. This paper presents the basic models for bounding ASF as well as the data analysis to test the assumptions and

performance of the bound model. The analysis is meant to provide a methodology for demonstrating the integrity of the ASF model for aviation. In particular, we focus on the weather model since it can be produced at a higher resolution.

The analysis shows that the weather model can and does bound the effect of ASF. In the range domain, it generally meets the conditions sufficient for bounding the ASF variation. The model provides bounds for the correlated and uncorrelated ASF variation that are conservative. This is partly validated by examining the division of the variation into uncorrelated and correlated portions. While the results show a few exceptions, the source of the exception is attributable to phenomena other than ASF. Position domain performance is exhibited and position errors are always overbounded. In fact, the data suggests that there is sufficient margin to accept reasonable errors in ASF estimates. While there is still not enough data to certify integrity, the analysis provides significant confidence in the use of the model. It leads to a methodology to demonstrating its integrity.

DISCLAIMER

The views expressed herein are those of the authors and are not to be construed as official or reflecting the views of the U.S. Coast Guard, Federal Aviation Administration, Department of Transportation or Department of Homeland Security or any other person or organization.

ACKNOWLEDGMENTS

The authors gratefully acknowledge the support of the Federal Aviation Administration and Mr. Mitchell Narins under Cooperative Agreement 2000-G-028. They are grateful for their support of Loran and the activities of the LORIPP.

The authors would also like to acknowledge the help and cooperation of the members of the LORIPP, who have all contributed to this work.

REFERENCES

[1] FAA report to FAA Vice President for Technical Operations Navigation Services Directorate, “Loran’s Capability to Mitigate the Impact of a GPS Outage on GPS Position, Navigation, and Time Applications,” March 2004

[2] Lo, Sherman, et al., “Loran Availability and Continuity Analysis for Required Navigation Performance 0.3” Proceedings of GNSS 2004 – The European Navigation Conference, Rotterdam, The Netherlands, May 2004

[3] Lo, Sherman et. al., “Loran Integrity Analysis for Required Navigation Performance 0.3”, Proceedings of the 5th International Symposium on Integration of LORAN-C/Eurofix and EGNOS/Galileo, Munich, Germany, June 2004

[4] Wenzel, Robert, Morris, Peter, and Montgomery, Kirk, “An Examination of Loran Signal Propagation Temporal Variation Modeling”, Proceedings of the International Loran Association 35th Annual Meeting, Groton, CT, October 2006

[5] Johler, J. R., Doherty, R. H., and Campbell, L. W., “Loran-C System Dynamic Model, Temporal Propagation Variation Study,” DOT-CG-D57-79, July 1979

[6] Lo, Sherman, et al., “Analysis of ASF for Required Navigation Performance 0.3”, Proceedings of the International Loran Association 32nd Annual Meeting, Boulder, CO, November 2003

[7] Slagle, D. C. and Wenzel, R. J., “Loran-C Signal Stability Study: NEUS/SEUS”, USCG CG-D-28-83, August 1983

[8] Taggart, D. S. and Slagle, D. C., “Loran-C Signal Stability Report: West Coast,” USCG CG-D-4-87, December 1986

[9] Samaddar, S. N., “Weather Effect on LORAN-C Propagation”, Navigation: Journal of the Institute of Navigation, Vol. 27, No. 1 Spring 1980, pp. 39-53

[10] Lo, Sherman, et. al., "Using Seasonal Monitor Data to Assess Aviation Integrity", Proceedings of the International Loran Association 36th Annual Meeting, Orlando, FL, October 2007

[11] Swaszek, Peter, et. al., “An Investigation into the Temporal Correlation at the ASF Monitor Sites”, Proceedings of the International Loran Association 36th Annual Meeting, Orlando, FL, October 2007

[12] Lo, Sherman, Peterson, Benjamin and Enge, Per “Proving the Integrity of the Weighted Sum Squared Error (WSSE) Loran Cycle Confidence Algorithm”, Proceedings of the Institute of Navigation National Technical Meeting, San Diego, CA, January 2007